Available online at www.sciencedirect.com
SCIENCE DIRECT
European Journal of Medicinal Chemistry 41 (2006) 745–755
EUROPEAN JOURNAL OF MEDICINAL CHEMISTRY
http://france.elsevier.com/direct/ejmech

Original article

Solid-phase synthesis and pharmacological evaluation of a library of peptidomimetics as potential farnesyltransferase inhibitors: an approach to new lead compounds

P. Gilleron [a], R. Millet [a], R. Houssin [a], N. Wlodarczyk [a], A. Farce [b], A. Lemoine [a]
J.-F. Goossens [a], P. Chavatte [b], N. Pommery [a], J.-P. Hénichart [a,*]

[a] *Institut de chimie pharmaceutique Albert-Lespagnol, EA 2692, université de Lille-II, rue du professeur-Laguesse, BP 83, 59006 Lille, France*
[b] *Laboratoire de chimie thérapeutique, faculté des sciences pharmaceutiques et biologiques, université de Lille-II, rue du professeur-Laguesse, BP 83, 59006 Lille, France*

Received in revised form 16 March 2006; accepted 20 March 2006
Available online 02 May 2006

Abstract

Oncogenic Ras proteins whose activation is farnesylation by farnesyltransferase have been seen as important targets for novel anticancer drugs. Inhibitors of this enzyme have already been developed as potential anti-cancer drugs, particularly by rational design based on the structure of the CA_1A_2X carboxyl terminus of Ras. Synthesis of a peptidomimetics library via solid-phase synthesis using the Multipin™ method is described here. The most active hits on cellular assays were resynthesized and enzymatic activity was measured. Compounds **A1**, **A5** and **A7** present significant activity on the isolated enzyme (IC_{50} = 117, 57.3 and 28.5 nM) and their molecular docking in the active site of the enzyme provides details on key interactions with the protein.

Keywords: Farnesyltransferase; Inhibitors; Peptidomimetics; Solid phase synthesis

1. Introduction

Cancer is an increasingly common disease for which treatments are not always selective of tumor cells. One of the possible targets would be to inhibit the function of the oncogene *ras* which is among the most frequently activating mutated genes in human tumors (30% on average, reaching up to 50% in colon cancer and up to 90% in pancreas cancer) [1,2]. Ras proteins play a key role in signal transduction pathway, cell growth and cell proliferation [3]. Activation of Ras proteins requires association to the plasma membrane which is mainly dependent on the attachment of a farnesyl (15-carbon) or of a geranylgeranyl (20-carbon) group to the cysteine residue located in a tetrapeptidic CA_1A_2X sequence at the carboxyl terminus of Ras proteins (A_1 and A_2: aliphatic amino acids; X: methionine or serine for farnesyltransferase, leucine or isoleucine for type I geranylgeranyltransferase) [4]. Inhibition of Zn-metalloenzyme farnesyltransferase (FTase) prevents membrane localization of Ras and so constitutes a valid target for the conception of new cytostatic anticancer drugs [5]. Farnesyltransferase inhibitors (FTIs) have thus been developed as a new class of extremely promising drugs for cancer treatment, either by rational design based on the structure of the CA_1A_2X carboxyl terminus of Ras or by random screening of chemical libraries or natural products [6,7]. Three of these inhibitors (Fig. 1) are being assessed in phase II/III of clinical trials [8,9]: R-115777 (for colorectal, non-small cell lung and breast cancers [10–12]), SCH-66336 and BMS-214662 (for leukemia [8,13]).

We report here the design and synthesis of a library of 64 peptidomimetics, potent specific inhibitors based on the structure of the CA_1A_2X sequence. The aim of this work was to rapidly discover new lead compounds. Compounds were prepared using solid-phase parallel synthesis by the Multipin™ method. These inhibitors were built on the basis of a zinc chelator linked to a selectivity factor (FTase vs. GGTase-I) by a spacer which correctly positioned these elements in the enzyme active site.

* Corresponding author. Tel.: +33 3 20 96 43 74; fax: +33 3 20 96 49 06.
E-mail address: jean-pierre.henichart@univ-lille2.fr (J.-P. Hénichart).

0223-5234/$ - see front matter © 2006 Elsevier SAS. All rights reserved.
doi:10.1016/j.ejmech.2006.03.017

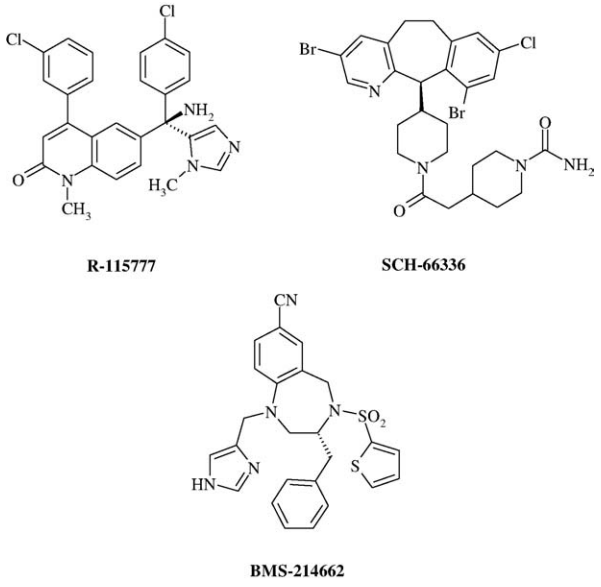

Fig. 1. Inhibitors in clinical trials.

Eight heterocycles **A**–**H** (Fig. 2) were chosen to vary the zinc chelator C of the CA_1A_2X box according to three criteria:

- Ability of nitrogen heterocycles, such as imidazole or pyridine, to coordinate the enzyme-bound zinc ion. Furan and thiophene were selected because of their property to maintain the enzymatic activity despite their lacking of metal coordination [14].
- Chemical opportunity: each compound possessed an aldehyde function in order to incorporate the spacer.
- Stability of compounds: our interest was focused on aromatic aldehydes generally more stable than hydroxamates or aliphatic aldehydes.

Seven of them (**B**–**H**) were commercially available whereas aldehyde **A** was synthesized according to a previously described procedure [15]. Besides these aldehydes, eight Fmoc-protected amino acids **1**–**8** (Fig. 3) were selected according to their diversity in varying the spacer A_1A_2 and their aliphatic, alicyclic or aromatic structure associated with their hydrophobic character required for enzyme recognition. These could be linear or branched so as to give either an extended conformation mimicking the position of the CA_1A_2X box in the substrate site or a bent conformation mimicking the location of

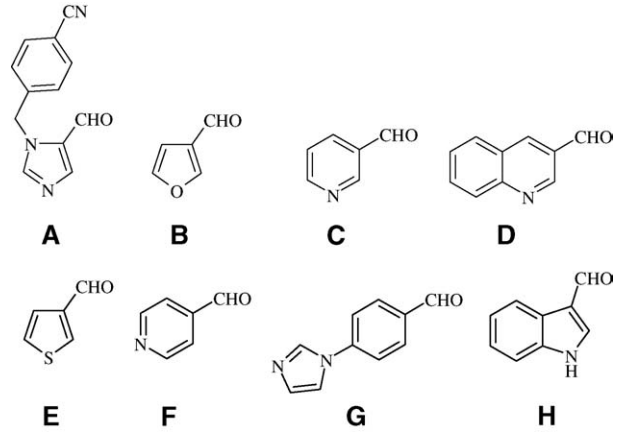

Fig. 2. Structure of aldehydes **A**–**H**.

the farnesylated molecule after moving the farnesyl moiety into the exit groove [16].

The terminal residue X was Phe-NH_2 which was more stable than Met-NH_2, prevented any risk of oxidation and allowed recognition by FTase or GGTase-I. In addition, amide group was found more effective than a C-terminal carboxylic function for cellular penetration of inhibitors, as found in one of our previous work.

2. Chemistry

Solid-phase peptide synthesis methodology is the quickest and most efficient way to prepare a library of peptidomimetics through parallel multi-step synthesis [17]. This method allows for limited purification difficulties.

The library of 64 compounds was built on a Geysen's pins apparatus (Chiron Multipin^{TM} method) [18,19]. The compounds were prepared as C-terminal amides using a Rink amide resin. Couplings on the pin apparatus were from the C- to the N-terminus (as is standard for solid phase peptide synthesis). The synthesis was performed according to the general reaction pathway outlined in Scheme 1.

So as to control the coupling of the two amino acids, the backbone amine (N-terminal position) was protected by an Fmoc residue which is stable with regard to acidic reagents and tertiary amines but can be readily cleaved under basic conditions. Fmoc deprotection and washing cycles were performed between each step. Fmoc deprotection of the pins using piperidine (compound **9**) was followed by coupling Fmoc-(*S*)-Phe-

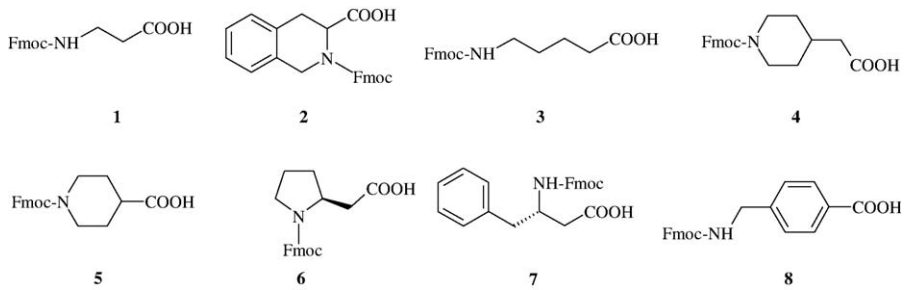

Fig. 3. Structure of protected amino acids **1**–**8**.

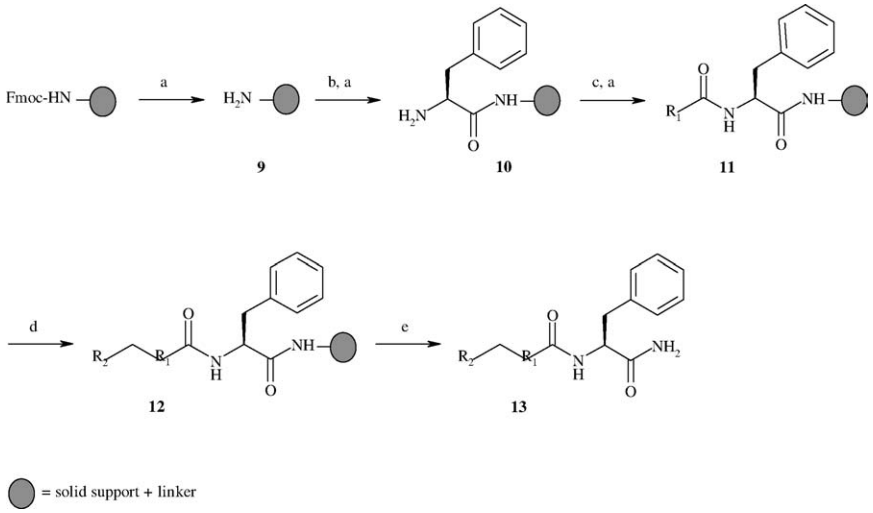

Scheme 1. Reagents and conditions: (a) Piperidine/DMF (1:4), 20 min; (b) Fmoc-(*S*)-Phe-OH, HBTU, DIEA, DMF, 6 h; (c) Fmoc-R_1-OH (**1**–**8**, see Fig. 3), HBTU, DIEA, DMF, 6 h; (d) i. R_2-CHO (**A**–**H**, see Fig. 2), MeOH, 2 h; ii. $NaBH_3CN$, 16 h; (e) TFA/H_2O/CH_2Cl_2/thioanisole/anisole/EDT (45:1:1:1:1:1), 3 h.

OH with the amino resin residue using standard HBTU coupling methodology. Removal of the Fmoc protecting group gave intermediate **10**. The second amino acid Fmoc-R_1-OH (**1**–**8**) was introduced using the same coupling method. After Fmoc deprotection giving **11**, the final step consisted in the introduction of the heterocycle R_2 via reductive amination of its appended aldehyde function (R_2-CHO, compounds **A**–**H**) and gave the solid-phase compound **12**. This reaction was carried out using a two-step procedure to limit the formation of the disubstituted amine: i) reaction between amine and aldehyde to give imine ii) reduction by $NaBH_3CN$. The reaction was optimized by varying several parameters: i) aldehyde concentration (10–500 mmol l^{-1}) ii) reaction time (30–180 min) iii) solvent polarity (MeOH or CH_2Cl_2/DMF) and iv) pH (by adding CH_3COOH or diisopropylethylamine). The best conversion rates were observed when aldehyde concentration was 200 mmol l^{-1}, reaction time was 2 h, solvent was MeOH and pH was that of the methanolic solution. Apart from **A1**, formation of the by-product resulting from double reductive amination could be explained by adsorption of the aldehyde on the resin.

TFA (in the presence of scavengers) mediated cleavage of peptidomimetic **12** from the resin and gave dipeptide **13** as C-terminal amide. Purity of each dipeptide was checked by LC-MS analysis (> 80% purity). Peptidomimetics synthesized with this method proved to be suitable for biological studies.

The whole library was tested for antiproliferative activity on L1210 (murine leukemia) and DU145 (prostate) cell lines. Only eight molecules showed inhibition > 80% at 100 μM on L1210 or DU145: compounds **A1**, **A5**–**A7**, **D7**, **E7**, **G7**, **H7** were selected for solution-phase resynthesis on a larger scale and for additional biological assessment (Fig. 4).

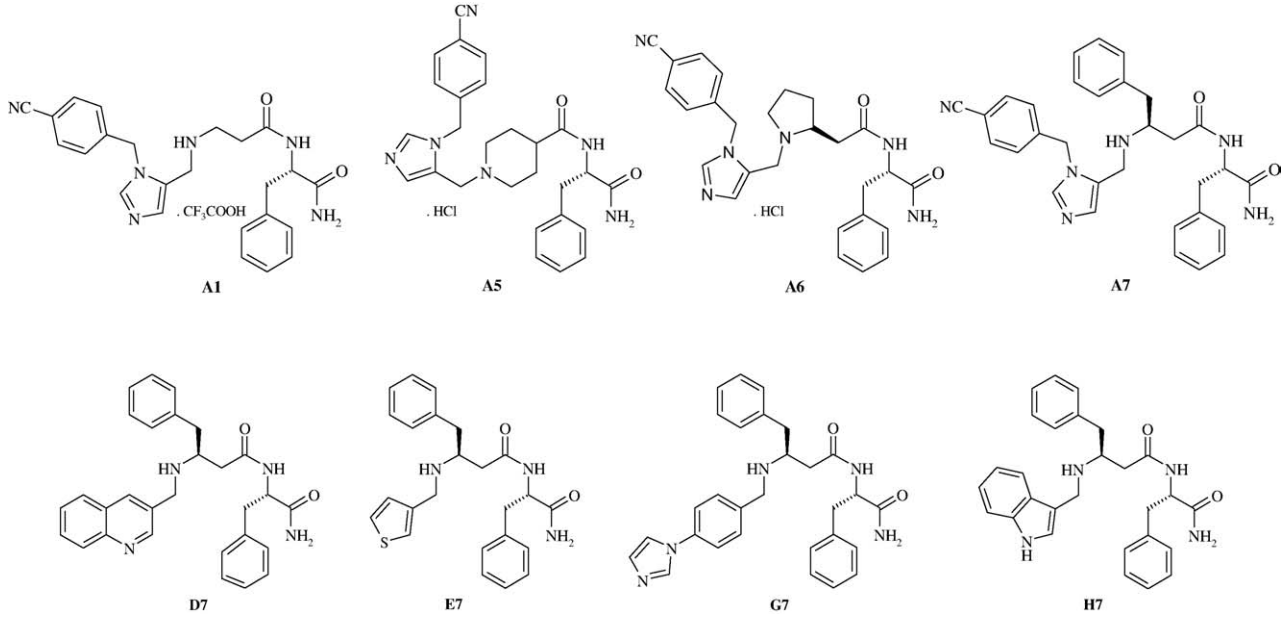

Fig. 4. Structure of compounds **A1**, **A5**–**A7**, **D7**, **E7**, **F7**, **G7**.

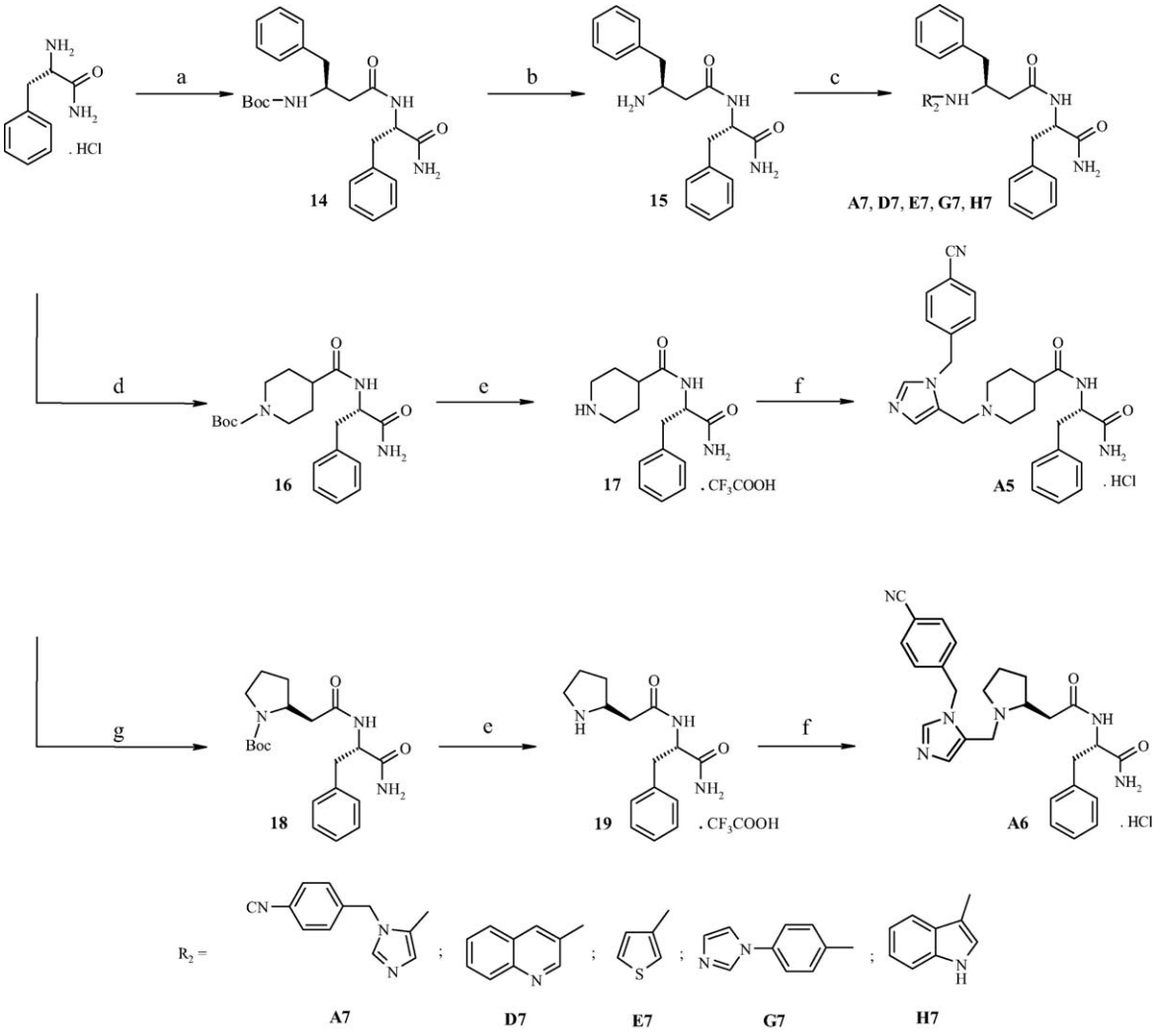

Scheme 2. Reagents and conditions: (a) Boc-(*S*)-β-homoPhe-OH, PyBOP, DIEA, CH_2Cl_2, rt, 16 h, 65%; (b) i. HCl/Et_2O, MeOH, rt, 4 h; ii. 10% $NaHCO_3$, 90%; (c) R_2-CHO (**A**, **D**, **E**, **G** or **H**, see Fig. 2), $NaBH_3CN$, MeOH, 3 Å molecular sieves, rt, 16 h, 20–50%; (d) Isonipecotic acid, HBTU, HOBt, DIEA, CH_2Cl_2, rt, 16 h, 80%; (e) TFA/CH_2Cl_2 (1:1), rt, 4 h, 95%; (f) i. 1-(4-Cyanobenzyl)-5-formylimidazole, TEA, $NaBH_3CN$, MeOH, 3 Å molecular sieves, 50 °C, 16 h; ii. HCl/isopropanol, 48–60%; (g) Boc-(*S*)-β-homoproline, HBTU, HOBt, DIEA, CH_2Cl_2, rt, 16 h, 86%.

The solution-phase synthesis of the selected compounds is illustrated on Scheme 2.

H-(*S*)-Phe-NH_2·(HCl) was coupled with Boc-(*S*)-β-homoPhe-OH, isonipecotic acid or Boc-(*S*)-β-homoPro to yield dipeptides **14**, **16** or **18**. The Boc protecting group was removed under standard conditions (HCl or TFA) and the resulting amines were subjected to reductive amination with aldehydes **A**, **D**, **E**, **G** or **H** to give final compounds **A5**–**A7**, **D7**, **E7**, **G7** or **H7**.

Another synthetic pathway was considered for the synthesis of **A1** (Scheme 3) since its isolation and purification failed using the previous synthesis strategy.

H-(*S*)-β-Ala-OMe·HCl was then subjected to reductive amination with 1-cyanobenzyl-1*H*-5-formylimidazole **A** to give secondary amine **20**. After protection of amine as carbamate (Boc) and saponification of the ester function of **21** with 2 N aqueous NaOH, carboxylic acid **22** was coupled with H-(*S*)-Phe-NH_2 to produce amide **23**; the final deprotection of amine (TFA) provided compound **A1**.

3. Results and discussion

The eight resynthesized compounds were tested for their ability to inhibit FTase catalyzed transfer of the FPP moiety to dansyl-CVIM and GGTase-I (which catalyses the transfer of the GGPP moiety to dansyl-GCVLL) [20,21]. This assay was performed by fluorescence spectrometry using rat brain cytosol fractions as an enzyme source [22]. Cellular proliferation was investigated on L1210, DU145, PC3 and LNCaP cells. Their biological activities are summarized in Tables 1 and 2.

Compounds **A1**, **A5** and **A7** inhibit FTase at submicromolar concentrations and exhibit good selectivity against GGTase-I. **A1** blocks growth of L1210, DU145 and PC3 cells at micromolar concentrations, **A7** blocks growth of L1210 and LNCaP in the same concentration range and **A5** is the most potent compound on L1210 cellular assay with an IC_{50} of 42.25 μM.

The best enzymatic activities were observed with 1-(4-cyanobenzyl)-5-methylimidazole containing compounds. This

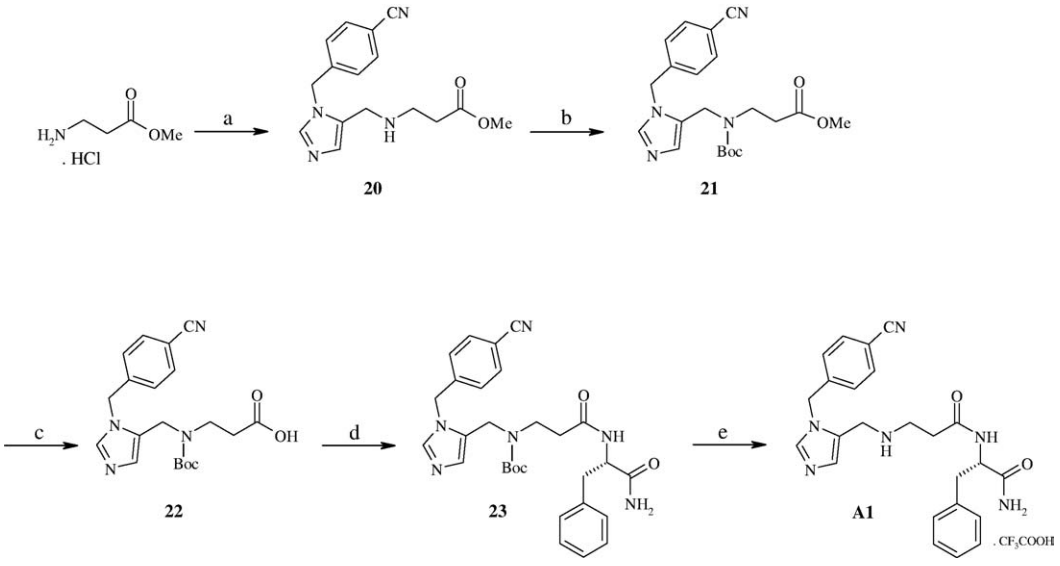

Scheme 3. Reagents and conditions: (a) 1-(4-Cyanobenzyl)-5-formylimidazole, TEA, $NaBH_3CN$, MeOH, 3 Å molecular sieves, rt, 16 h, 65%; (b) $(Boc)_2O$, 2 N NaOH, dioxane/H_2O 4:1, rt, 16 h, 30%; (c) i. 2 N NaOH, MeOH, rt, 3 h; ii. 1 N HCl, 60%; (d) H-(*S*)-Phe-NH_2•HCl, HBTU, HOBt, DIEA, CH_2Cl_2, rt, 18 h, 62%; (e) TFA/CH_2Cl_2 (1:1), rt, 4 h, 98%.

confirmed previous results [15] where this heterocyclic group constituted an effective cysteine substitute for FTIs. No other heterocycle was found to have better enzymatic activity in binding Zn^{2+}.

Table 1
FTase and GGTase I activities [a] of compounds **A1**, **A5**–**A7**, **D7**, **E7**, **F7**, **G7**

Compound	IC_{50} (nM)		K_{app} (nM)
	FTase	GGTase-I	
A1	117 ± 10	> 40 000	123 ± 11
A5	57.3 ± 9.0	nd [b]	nd [b]
A6	nd [b]	nd [b]	nd [b]
A7	28.5 ± 4.2	> 40 000	54.5 ± 9.2
D7	1200 ± 112	nd [b]	nd [b]
E7	> 40 000	nd [b]	nd [b]
G7	328 ± 21	> 40 000	nd [b]
H7	254 ± 18	> 40 000	nd [b]

[a] Data are given as mean ± S.E.M. of three independent experiments.
[b] Not determined.

Table 2
Biological activities [a] of compounds **A1**, **A5**–**A7**, **D7**, **E7**, **F7**, **G7** on cell growth

Compound	IC_{50} (μM) or % inhibition [b]			
	L1210	DU145	PC3	LNCaP
A1	11%	5%	4%	ns [c]
A5	42.25	ns [c]	ns [c]	nd [d]
A6	3%	nd [d]	nd [d]	nd [d]
A7	41%	ns [c]	ns [c]	27%
D7	14%	ns [c]	5%	38%
E7	10%	39%	ns [c]	15%
G7	17%	33%	ns [c]	17%
H7	31%	11%	14%	11%

[a] Data are given as mean ± S.E.M. of three independent experiments.
[b] Compounds tested at the concentration of 10 μM.
[c] Not significant.
[d] Not determined.

The inhibition of compound **A7** with a β-homoPhe spacer was four times more potent (IC_{50} = 28.5 nM) than that of **A1** with a β-Ala spacer (IC_{50} = 117 nM). Thus, a supplementary benzyl group led to an increase in FTase inhibition which can be explained by its satisfactory position and favorable interactions on the FTase active site. Moreover, inhibitors **A1** and **A7** exhibited their competitive nature (Table 1).

Finally, molecular docking, using the modeling program GOLD, was performed to study the interaction of the most potent compounds **A1**, **A5** and **A7** (Figs. 5–7) with the enzyme and to provide a reasonable explanation for the inhibitory activity of these structures.

In addition to coordination observed between the distal nitrogen of imidazole and Zn^{2+} used as starting fragments for this

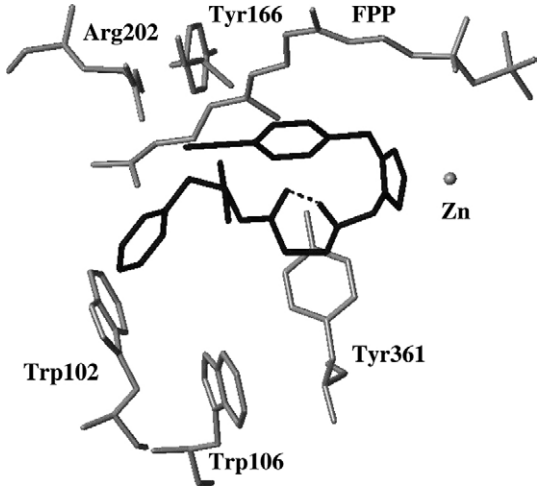

Fig. 5. Docking of inhibitor **A1** (in black) in the FTase binding site. The FPP, Arg202β, Tyr166α and the hydrophobic pocket defined by the aromatic side chains of Trp102β, Trp106β, Tyr361β are shown in grey. The hydrogen bond between N–H and C=O is highlighted by a dotted line.

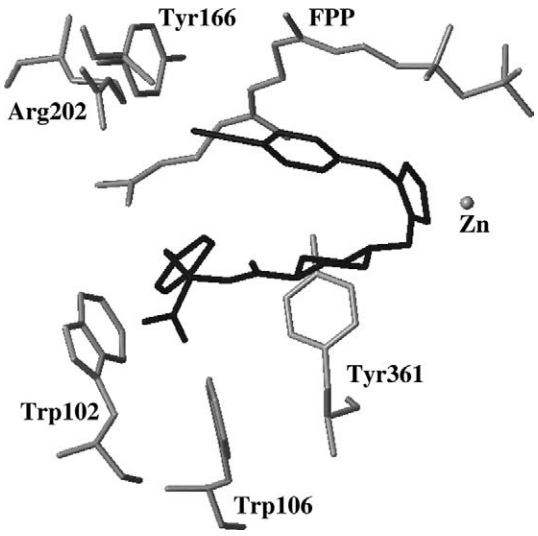

Fig. 6. Docking of inhibitor **A5** (in black) in the FTase binding site. The FPP, Arg202β, Tyr166α and the hydrophobic pocket defined by the aromatic side chains of Trp102β, Trp106β, Tyr361β are shown in grey.

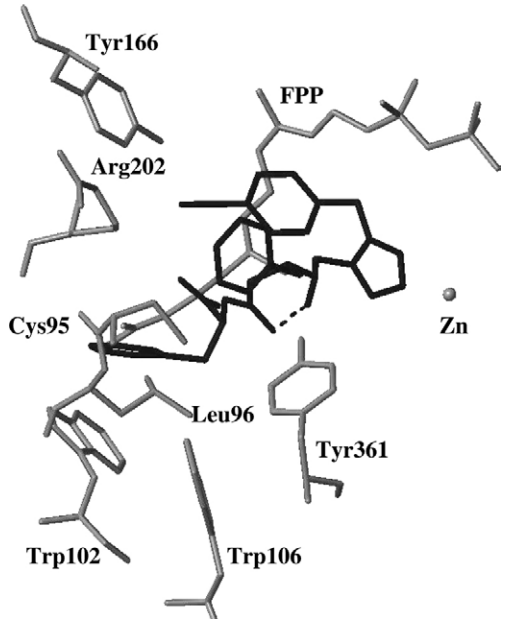

Fig. 7. Docking of inhibitor **A7** (in black) in the FTase binding site. The FPP, Arg202β, Tyr166α, Cys95β, Leu96β and the hydrophobic pocket defined by the aromatic side chains of Trp102β, Trp106β, Tyr361β are shown in grey. The hydrogen bond between N–H and C=O is highlighted by a dotted line.

study, docking revealed an interaction between Phe-NH_2 and a hydrophobic pocket, called the A_2 binding site, delineated by Trp102β, Trp106β and Tyr361β in the β-subunit [23]. The X residue was positioned in the hydrophobic pocket where the A_2 residue fits: **A1**, **A5** and **A7** constituted three mimetic inhibitors of the CA_1A_2 sequence. This study also revealed an additional interaction between the **A7** homoPhe spacer and the exit groove (partly defined by Cys95β and Leu96β) that could enhance inhibitory activity. Docking also revealed a hydrogen bonding between the secondary amine and the amide oxygen of these compounds **A1** and **A7**, giving the molecules a pseudocyclic conformation, as does the piperidinic residue in **A5**, and then satisfactorily positioning the aryl residue of Phe-NH_2 in the A_2 binding site and favoring the fit of the supplementary benzyl of **A7** in the exit groove. No interaction of the C-terminal amide residue with the active site was observed.

A1, **A5** and **A7** contained respectively a β-Ala, a piperidinyl or an (*S*)-β-homoPhe spacer. Thus, these scaffolds constitute interesting patterns to position the FTase recognition elements in the FTase binding site. These results could be used to design new FTIs to improve enzymatic and cellular activities.

4. Conclusion

We have reported herein the preparation of a library of potent CA_1A_2X-based FTIs using parallel solid-phase synthesis. Multipin™ methodology proved to be a very convenient method for parallel multi-step synthesis. Although these peptidomimetics are unlikely to be drug candidates themselves, they could be valuable leads for developing new FTIs. This CA_1A_2X-based library provides an interesting new tool to improve structure-activity relationships and thus to propose new efficient structures. We identified three molecules, **A1**, **A5** and **A7**, containing respectively a β-Ala, a piperidinyl or an (*S*)-β-homoPhe spacer. Optimization of these hits through non-peptidic inhibitors will be described in a future paper.

Recently, protein farnesylation has been identified in trypanosomatids and in the malaria parasite; FTIs have been shown to be toxic towards these parasites [24,25]. Results of antiparasitic activity on the chloroquine-resistant FcB1R strain of *Plasmodium falciparum* revealed no significant activity for the components of this library. In vitro antiplasmodial activity was determined using a previously described assay [26].

Recent studies have, however, suggested that the cytotoxic actions of FTIs are not exclusively due to the inhibition of Ras proteins and have indicated that other farnesylated protein targets, other than Ras, have to be considered [27,28]. These candidate targets include other Ras-family GTPases such as RhoB [29] and Rheb [30], the centromere-binding proteins CENP-E and CENP-F [31,32], the phosphatases PRL-1, -2 and -3, [33] or an unidentified protein that functions as activator of the PI3-K/Akt pathway [34]. These arguments may explain the observed discordance between the enzymatic and cellular activities of the inhibitors described here.

5. Experimental protocols

5.1. Chemistry

SynPhase™ crowns, deepwell microtiter plates (8 × 12), and Multipin™ stems were purchased from Chiron Technologies (San Diego, CA). Analytical thin-layer chromatography was performed on precoated Kieselgel $60F_{254}$ plates from Merck; the spots were located by UV (254 and 366 nm). Silica gel 60 (230–400 mesh) purchased from Merck was used for column chromatography. The structures of resynthesized compounds were supported by IR (FT-Bruker Vector 22 instrument, neat) and by ^{1}H NMR at 300 MHz (Bruker DRX-300

spectrometer). Chemical shifts were reported in ppm using tetramethylsilane as a standard, *J* values are in hertz, and the splitting patterns were designated as follows: s, singlet; d, doublet; t, triplet; q, quadruplet; m, multiplet; bs, broad singlet; dd, doublet of doublet. Melting points were determined with a Büchi 530 capillary melting point apparatus and remain uncorrected. Mass spectra were recorded on a quadripolar Finnigan Mat SSQ 710 instrument. Elemental analyses of resynthesized compounds were performed by the "Service Central d'Analyses" at the CNRS, Vernaison (France).

5.1.1. Library solid-phase synthesis

Solid-phase synthesis was performed using SynPhase™-MD (methacrylic acid/dimethylacrylamide) I-series crowns (pins) derivatized with Fmoc-protected rink amide linkers. The 64 products were synthesized in deepwell microtiter plates (8 × 12) using Multipin™ stems to support the pins. Peptidomimetic synthesis was carried out at room temperature without agitation. The following standard purification and deprotection procedures were used: the stems were suspended in a plastic wash bath, the attached pins were washed successively with DMF (3 × 5 min), MeOH (1 × 5 min) and CH_2Cl_2 (3 × 5 min) and the pins were then air-dried to give the solid-phase intermediates. Deprotection of the Fmoc protected amines was obtained using 25% piperidine in DMF for 20 min. After deprotection and purification of 64 pins by the standard procedure, the first coupling of Fmoc-(*S*)-Phe-OH was achieved by immersing each pin in the well of a microtiter plate. Each well contained 400 μl of a DMF solution of Fmoc-(*S*)-Phe-OH (120 mmol l^{-1}), HBTU (120 mmol l^{-1}), and DIEA (144 mmol l^{-1}). After 6 h, the pins were removed from the microtiter wells, washed by the standard procedure and allowed to air-dry. The pins were deprotected following the above conditions, washed and allowed to air-dry. The second coupling reaction and deprotection were performed using the same methodology. Each pin was then immersed in a microtiter plate wherein each well contained 400 μl of a solution of the appropriate Fmoc-(*S*)-amino acid **1**–**8** (120 mmol l^{-1}), HBTU (120 mmol l^{-1}) and DIEA (144 mmol l^{-1}) in DMF. After 6 h, the pins were removed from the microtiter wells and deprotected by washing and air-drying. The pins were deprotected using the above conditions, washed and allowed to air-dry. Reductive amination was then obtained by immersing each pin in a microtiter plate wherein each well contained 400 μl of an MeOH solution of the appropriate aldehyde **A**–**H** (200 mmol l^{-1}). After 2 h, the pins were removed from the microtiter wells, washed with MeOH (3 × 5 min), CH_2Cl_2 (2 × 5 min) and allowed to air-dry. The pins were then immersed in 400 μl of an MeOH solution of $NaBH_3CN$ (240 mg in 30 ml MeOH). After 16 h, the pins were removed from the microtiter plate, washed with MeOH (3 × 5 min), CH_2Cl_2 (2 × 5 min), and allowed to air-dry. The peptidomimetics were cleaved from the pins using TFA/H_2O/CH_2Cl_2/thioanisole/anisole/1,2-ethanedithiol (90:2:2:2:2:2) for 3 h, and the solvents were removed under reduced pressure. A solvent mixture containing Et_2O/petroleum ether (1:2) was added to each well, the solutions were centrifuged, and the solvents were decanted. LC-MS were recorded for all the products. The corresponding molecular ion was observed for each peptidomimetic, and the HPLC indicated one major product in each case.

5.1.2. Compounds resynthesized in solution-phase for biological evaluation

*5.1.2.1. N-tert-butoxycarbonyl-(S)-β-homoPhe-(S)-Phe-NH_2 (**14**)*. Diisopropylethylamine (1.90 ml, 10.7 mmol) and PyBOP (2.79 g, 5.37 mmol) were added to a solution of Boc-(*S*)-β-homoPhe-OH (1 g, 3.58 mmol) in 50 ml of dry CH_2Cl_2 at room temperature. After 2 h, H-(*S*)-Phe-NH_2·HCl (719 mg, 3.58 mmol) was added and the mixture was stirred for 16 h at room temperature. The solvent was then removed under reduced pressure. The residue was dissolved in AcOEt and washed with 5% aqueous $NaHCO_3$, 0.25 N HCl and H_2O. The organic layer was dried over $MgSO_4$ and the solvent was evaporated. The residue was triturated with CH_2Cl_2/Et_2O (1:1) and the white solid was filtered and dried to give **14** (65%). m. p. 180–181 °C; IR (cm^{-1}): 1687, 1677, 1647; ^1H NMR (DMSO-d_6): 1.39 (s, 9H), 1.72 (m, 2H), 2.48–2.52 (m, 1H), 2.80–2.87 (m, 1H), 2.99–3.03 (m, 1H), 3.32–3.34 (m, 1H), 3.80–3.83 (m, 1H), 4.43–4.49 (m, 1H), 7.12–7.29 (m, 12H), 7.41 (s, 1H), 7.78 (d, $J = 8.2$ Hz, 1H); MS (CI): 426 (MH^+). Anal. ($C_{24}H_{31}N_3O_4$) C, H, N.

*5.1.2.2. H-(S)-β-homoPhe-(S)-Phe-NH_2 (**15**)*. An HCl-saturated Et_2O solution was added to a solution of carbamate **14** (1 g, 2.35 mmol) in 20 ml of MeOH. The mixture was stirred for 4 h at room temperature, and the solvent evaporated. The residue was dissolved in 10% aqueous $NaHCO_3$ and extracted with AcOEt. The organic layer was dried over $MgSO_4$ and evaporated to give **15** as a colorless oil (90%). IR (cm^{-1}): 3393, 1632; ^1H NMR ($CDCl_3$): 1.69–1.71 (m, 2H), 1.96–2.08 (m, 2H), 2.52–2.57 (m, 2H), 2.81–3.08 (m, 1H), 3.14–3.16 (m, 1H), 3.19–3.38 (m, 1H), 4.63–4.70 (m, 1H), 5.48 (s, 1H), 6.20 (s, 1H), 7.12–7.31 (m, 10H), 7.88 (d, $J = 7.8$ Hz, 1H), MS (CI): 326 (MH^+). Anal. ($C_{19}H_{23}N_3O_2$) C, H, N.

*5.1.2.3. General procedure for the synthesis of **A7**, **D7**, **E7**, **G7** and **H7**.* Molecular sieves (3 Å) and $NaBH_3CN$ (0.55 mmol) were added to a stirred solution of amine **15** (0.2 g, 0.55 mmol) and appropriate aldehyde **A**, **D**, **E**, **G** or **H** (0.44 mmol) in 30 ml of dry MeOH. The reaction mixture was stirred at room temperature for 16 h in a dry nitrogen atmosphere. The molecular sieves were filtered off and the solvent was removed under reduced pressure. The residue was dissolved in AcOEt and washed successively with 5% aqueous $NaHCO_3$, H_2O and brine. The organic layer was dried over $MgSO_4$ and evaporated. The residue was purified by column chromatography (CH_2Cl_2/MeOH 9:1).

*5.1.2.3.1. [N-(4-cyanobenzyl-5-imidazolylmethyl)]-(S)-β-homoPhe-(S)-Phe-NH_2 (**A7**)*. White solid; yield 50%; m.p. 61–62 °C; IR (cm^{-1}): 2229, 1654; ^1H NMR (DMSO-d_6): 2.32–2.40 (m, 2H), 2.72–2.91 (m, 2H), 3.01–3.28 (m, 2H), 3.54–3.59 (m, 2H), 4.28–4.33 (m, 1H), 4.53–4.65 (m, 1H),

5.35 (s, 2H), 6.68 (s, 1H), 6.81–7.85 (m, 18H), 8.02 (d, $J = 9.1$ Hz, 1H); MS (CI): 521 (MH^+). Anal. ($C_{31}H_{32}N_6O_2$) C, H, N.

*5.1.2.3.2. [N-(3-quinolylmethyl)]-(S)-β-homoPhe-(S)-Phe-NH$_2$ (**D7**)*. White solid; yield 20%; m.p. 273–274 °C; IR (cm^{-1}): 3312, 1644; ^{1}H NMR (DMSO-d_6): 2.77–2.83 (m, 2H), 3.18–3.22 (m, 2H), 3.30–3.37 (m, 2H), 3.60–3.69 (m, 2H), 4.20–4.26 (m, 1H), 4.65–4.75 (m, 1H), 7.40–8.10 (m, 18H), 8.20 (d, $J = 8.2$ Hz, 1H), 8.81 (s, 1H); MS (CI): 466 (MH^+). Anal. ($C_{29}H_{30}N_4O_2$) C, H, N.

*5.1.2.3.3. [N-(3-thienylmethyl)]-(S)-β-homoPhe-(S)-Phe-NH$_2$ (**E7**)*. White solid; yield 20%; m.p. 75–76 °C; IR (cm^{-1}): 3312, 1649; ^{1}H NMR (DMSO-d_6): 2.35–2.60 (m, 2H), 2.72–2.88 (m, 2H), 2.89–3.07 (m, 2H), 3.35–3.42 (m, 3H), 4.45–4.72 (m, 1H), 7.10–7.25 (m, 14H), 7.44–7.64 (m, 2H), 8.10 (d, $J = 8.0$ Hz, 1H); MS (EI): 421 (M^+). Anal. ($C_{24}H_{27}N_3O_2S$) C, H, N.

*5.1.2.3.4. {N-[4-(1H-imidazol-1-yl)benzyl]}-(S)-β-homoPhe-(S)-Phe-NH$_2$ (**G7**)*. Yellow solid; yield 40%; m.p. 166–167 °C; IR (cm^{-1}): 3301, 1666, 1635; ^{1}H NMR (DMSO-d_6): 2.30–2.51 (m, 2H), 2.75–2.86 (m, 2H), 2.89–3.07 (m, 2H), 3.21–3.35 (m, 1H), 3.45–3.58 (m, 2H), 4.57–4.73 (m, 1H), 6.96–7.82 (m, 20H), 8.10 (d, $J = 8.2$ Hz, 1H); MS (CI): 482 (MH^+). Anal. ($C_{29}H_{31}N_5O_2$) C, H, N.

*5.1.2.3.5. {N-[(1H-indol-3-ylmethyl)]}-(S)-β-homoPhe-(S)-Phe-NH$_2$ (**H7**)*. Brown solid; yield 35%; m.p. 187–189 °C; IR (cm^{-1}): 1664, 1633; ^{1}H NMR (DMSO-d_6): 2.28–2.49 (m, 2H), 2.68–2.87 (m, 2H), 2.91–3.07 (m, 2H), 3.27–3.38 (m, 1H), 3.83–3.98 (m, 2H), 4.49–4.68 (m, 1H), 7.11–7.92 (m, 19H), 8.07 (d, $J = 8.2$ Hz, 1H); MS (CI): 455 (MH^+). Anal. ($C_{28}H_{30}N_4O_2$) C, H, N.

*5.1.2.4. General procedure for the synthesis of carbamates **16** and **18***. Diisopropylethylamine (4.5 ml, 26.2 mmol), HBTU (4.97 g, 13.1 mmol) and HOBt (590 mg, 4.36 mmol) were added to a solution of isonipecotic acid or Boc-(*S*)-β-homoPro (8.72 mmol) in 60 ml of dry CH_2Cl_2. After 2 h, H-(*S*)-Phe-NH_2·HCl (1.75 g, 8.72 mmol) was added and the mixture was stirred for 16 h at room temperature. The salts were filtered off and the filtrate was washed with 0.1 N HCl, H_2O and brine. The organic layer was dried over $MgSO_4$ and the solvent was then removed under reduced pressure. The residue was purified by column chromatography (CH_2Cl_2/MeOH 49:1).

*5.1.2.4.1. 1-tert-Butoxycarbonylpiperidine-4-carbonyl-(S)-Phe-NH$_2$ (**16**)*. White solid; yield 80%; m.p. 165–166 °C; IR (cm^{-1}): 1685, 1670, 1636; ^{1}H NMR ($CDCl_3$): 1.46 (s, 9H), 1.51–1.53 (m, 1H), 1.56–1.62 (m, 1H), 2.17–2.30 (m, 1H), 2.66–2.74 (m, 2H), 2.99–3.22 (m, 3H), 3.66–3.76 (m, 1H), 4.02–4.11 (m, 2H), 4.71 (q, $J = 7.3$ Hz, 1H), 5.79 (bs, 1H), 6.33 (bs, 1H), 6.52 (d, $J = 8.5$ Hz, 1H), 7.19–7.33 (m, 5H); MS (CI): 376 (MH^+). Anal. ($C_{20}H_{29}N_3O_4$) C, H, N.

*5.1.2.4.2. 1-tert-Butoxycarbonyl-(S)-β-homoPro-(S)-Phe-NH$_2$ (**18**)*. White solid; yield 86%; m.p. 96–97 °C; IR (cm^{-1}): 1682, 1680, 1633; ^{1}H NMR ($CDCl_3$): 1.46 (s, 9H), 1.50–2.25 (m, 4H), 2.55–2.65 (m, 2H), 2.90–3.12 (m, 2H), 3.18–3.35 (m, 2H), 3.98–4.15 (m, 1H), 4.70–4.78 (m, 1H), 5.90 (bs, 1H), 6.78 (bs, 2H), 7.19–7.35 (m, 5H); MS (CI): 376 (MH^+). Anal. ($C_{20}H_{29}N_3O_4$) C, H, N.

*5.1.2.5. General procedure for the preparation of amines **17** and **19***. Carbamate **16** or **18** was dissolved in 20 ml of a solution of TFA/CH_2Cl_2 (1:1). The reaction mixture was stirred at room temperature for 4 h. The solvent was then evaporated. The residue was triturated in Et_2O and the solid was filtered and dried.

*5.1.2.5.1. Piperidine-4-carbonyl-(S)-Phe-NH$_2$ trifluoroacetate (**17**)*. White solid; yield 95%; m.p. 206–207 °C; IR (cm^{-1}): 1672, 1640; ^{1}H NMR (DMSO-d_6): 1.38–1.50 (m, 1H), 1.61–1.79 (m, 3H), 2.39–2.47 (m, 1H), 2.69–2.90 (m, 3H), 3.00–3.07 (m, 1H), 3.13–3.26 (m, 2H), 4.41–4.49 (m, 1H), 7.09 (s, 1H), 7.17–7.28 (m, 5H), 7.52 (s, 1H), 8.11 (d, $J = 8.8$ Hz, 1H), 8.34 (bs, 1H), 8.69 (bs, 1H); MS (CI): 276 (MH^+). Anal. ($C_{15}H_{21}N_3O_2$·CF_3COOH) C, H, N.

*5.1.2.5.2. (S)-H-β-homoPro-(S)-Phe-NH$_2$ trifluoroacetate (**19**)*. White solid; yield 95%; m.p. 198–200 °C; IR (cm^{-1}): 1680, 1643; ^{1}H NMR (DMSO-d_6): 1.60–1.90 (m, 4H), 2.45–2.70 (m, 4H), 3.18–3.30 (m, 2H), 3.45–3.62 (m, 1H), 4.45–4.55 (m, 1H), 7.15 (s, 1H), 7.18–7.30 (m, 5H), 7.56 (s, 1H), 8.42 (d, $J = 8.4$ Hz, 1H), 8.70 (bs, 1H), 9.02 (bs, 1H); MS (CI): 276 (MH^+). Anal. ($C_{15}H_{21}N_3O_2$·CF_3COOH) C, H, N.

*5.1.2.6. General procedure for the preparation of amines **A5** and **A6***. 1-Cyanobenzyl-5-formylimidazole (361 mg, 1.71 mmol), 3 Å molecular sieves were added to a stirred solution of amines **17** or **19** (2.57 mmol) and triethylamine (0.36 ml, 2.57 mmol) in 30 ml of dry MeOH before $NaBH_3CN$ was added (118 mg, 1.88 mmol) after 2 h at 50 °C in a dry nitrogen atmosphere. The reaction mixture was stirred at 50 °C for 16 h. The molecular sieves were filtered off and the solvents were removed under reduced pressure. The residue was dissolved in AcOEt and washed successively with 5% aqueous $NaHCO_3$, H_2O and brine. The organic layer was dried over $MgSO_4$ and evaporated. The residue was purified by column chromatography (CH_2Cl_2/MeOH 95:5) and hydrochloride was obtained by adding a 5–6 N isopropanolic HCl solution. The salt was then washed with Et_2O and AcOEt and dried.

*5.1.2.6.1. 1-{[1-(4-Cyanobenzyl)-1H-imidazol-5-yl]methyl}piperidine-4-carbonyl-(S)-Phe-NH$_2$ hydrochloride (**A5**)*. White solid; yield 60%; m.p. 235–237 °C; IR (cm^{-1}): 2237, 1673, 1628; ^{1}H NMR (DMSO-d_6): 1.69–1.78 (m, 2H), 2.05–2.12 (m, 2H), 2.59–2.77 (m, 4H), 3.00 (dd, $J = 6.5$ Hz, 1H), 3.16–3.20 (m, 2H), 3.36 (s, 2H), 4.39–4.49 (m, 1H), 5.34 (s, 2H), 7.05 (s, 1H), 7.19–7.28 (m, 5H), 7.43 (s, 1H), 7.53 (d, $J = 8.4$ Hz, 2H), 7.91 (d, $J = 8.5$ Hz, 2H), 8.15 (s, 1H), 8.64

(d, $J = 8.5$ Hz, 1H), 9.23 (s, 1H), 11.56 (bs, 1H); MS (CI): 471 (MH^+). Anal. ($C_{27}H_{30}N_6O_2 \cdot 2.5\ HCl \cdot 5\ H_2O$) C, H, N.

*5.1.2.6.2. 1-{[1-(4-Cyanobenzyl)-1H-imidazol-5-yl]methyl}-(S)-β-homoPro-(S)-Phe-NH_2 hydrochloride (**A6**).* White solid; yield 48%; m.p. 224–226 °C; IR (cm^{-1}): 2231, 1665, 1636; ^1H NMR (DMSO-d_6): 1.70–2.00 (m, 4H), 2.45–2.75 (m, 2H), 2.90–3.20 (m, 2H), 3.30–3.50 (m, 2H), 3.72–3.84 (m, 1H), 4.29–4.49 (m, 2H), 4.53–4.69 (m, 1H), 5.77 (s, 2H), 7.15–7.32 (m, 7H), 7.52 (d, $J = 8.4$ Hz, 2H), 7.91 (d, $J = 8.5$ Hz, 2H), 8.12 (s, 1H), 8.64 (d, $J = 8.5$ Hz, 1H), 9.22 (s, 1H), 11.73 (bs, 1H); MS (CI): 471 (MH^+). Anal. ($C_{27}H_{30}N_6O_2 \cdot 2\ HCl \cdot 3\ H_2O$) C, H, N.

*5.1.2.7. Methyl 3-({[1-(4-cyanobenzyl)-1H-imidazol-5-yl]methyl}-β-Ala-OMe (**20**).* 1-(4-Cyanobenzyl)-5-formylimidazole (3 g, 14.2 mmol) and 3 Å molecular sieves were added to a stirred solution of *H*-β-Ala-OMe·HCl (4.96 g, 35.5 mmol) and triethylamine (5 ml, 35.5 mmol) in 80 ml of dry MeOH, before $NaBH_3CN$ was added (983 mg, 15.6 mmol) after 2 h at room temperature in a dry nitrogen atmosphere. The reaction mixture was stirred at room temperature for 16 h. The molecular sieves were filtered off and the solvent was removed under reduced pressure. The residue was dissolved in AcOEt and washed successively with 5% aqueous $NaHCO_3$, H_2O and brine. The organic layer was dried over $MgSO_4$ and evaporated. The residue was purified by column chromatography (CH_2Cl_2/MeOH 95:5) to give **20** as a colorless oil (65%); IR (cm^{-1}): 2230, 1732; ^1H NMR ($CDCl_3$): 2.42 (t, $J = 6.0$ Hz, 2H), 2.81 (t, $J = 6.0$ Hz, 2H), 3.59 (s, 2H), 3.67 (s, 3H), 5.35 (s, 2H), 7.00 (s, 1H), 7.18 (d, $J = 8.2$ Hz, 2H), 7.52 (s, 1H), 7.63 (d, $J = 8.2$ Hz, 2H); MS (CI): 299 (MH^+). Anal. ($C_{16}H_{18}N_4O_2$) C, H, N.

*5.1.2.8. Methyl 3-[(tert-butoxycarbonyl)-3-{[1-(4-cyanobenzyl)-1H-imidazol-5-yl]methyl}-β-Ala-OMe (**21**).* Di-*tert*-butyl dicarbonate (1.65 g, 7.55 mmol) and 2 N aqueous NaOH (3.77 ml, 7.55 mmol) were added to a solution of amine **20** (1.5 g, 5.03 mmol) in 50 ml of a mixture dioxane/H_2O (4:1). The reaction mixture was stirred at room temperature for 16 h. The solvents were then evaporated, the residue was dissolved in AcOEt and washed with H_2O and brine. The organic layer was dried over $MgSO_4$ and concentrated under reduced pressure. The residue was purified by column chromatography (CH_2Cl_2/MeOH 96:4) to give **21** as a yellow oil (30%); IR (cm^{-1}): 2230, 1735, 1686; ^1H NMR ($CDCl_3$): 1.34 (s, 9H), 2.38–2.46 (m, 2H), 3.27–3.31 (m, 2H), 3.70 (s, 3H), 4.44 (s, 2H), 5.26–5.30 (m, 2H), 7.07–7.10 (m, 3H), 7.53–7.63 (m, 3H); MS (CI): 399 (MH^+). Anal. ($C_{21}H_{26}N_4O_4$) C, H, N.

*5.1.2.9. 3-[(tert-Butoxycarbonyl)-3-{[1-(4-cyanobenzyl)-1H-imidazol-5-yl]methyl}amino]-β-Ala-OH (**22**).* 2 N Aqueous NaOH (0.80 ml, 1.60 mmol) was added to a solution of ester **21** (320 mg, 0.80 mmol) in 5 ml of MeOH. The reaction mixture was stirred at room temperature for 3 h and then neutralized with 1 N aqueous HCl until pH 5–6. MeOH was evaporated and replaced by AcOEt. The mixture was acidified with 1 N aqueous HCl until pH 3–4 and the organic layer was extracted, dried over $MgSO_4$ and evaporated. The residue was purified by column chromatography (CH_2Cl_2/MeOH 9:1) to give **22** as a white solid (60%); m.p. 123–124 °C; IR (cm^{-1}): 3396, 2231, 1695, 1686; ^1H NMR ($CDCl_3$): 1.37 (s, 9H), 2.44–2.47 (m, 2H), 3.35–3.37 (m, 2H), 4.45 (s, 2H), 5.31–5.33 (m, 2H), 7.13–7.19 (m, 3H), 7.62–7.65 (m, 3H); MS (CI): 385 (MH^+). Anal. ($C_{20}H_{24}N_4O_4$) C, H, N.

*5.1.2.10. 3-[(tert-Butoxycarbonyl)-3-{[1-(4-cyanobenzyl)-1H-imidazol-5-yl]methyl}-β-Ala-(S)-Phe-NH_2 (**23**).* Diisopropylethylamine (0.27 ml, 1.56 mmol), HBTU (296 g, 0.78 mmol) and HOBt (35.1 mg, 0.26 mmol) were added to a solution of acid **22** (200 mg, 0.52 mmol) in 20 ml of dry CH_2Cl_2. After 2 h, H-(*S*)-Phe-NH_2·HCl (104 mg, 0.52 mmol) was added and the mixture was stirred for 18 h at room temperature. The salts were filtered off and the filtrate was washed with 0.1 N HCl, H_2O and brine. The organic layer was dried over $MgSO_4$ and the solvent was then removed under reduced pressure. The residue was purified by column chromatography (CH_2Cl_2/MeOH 91:9) to give **23** as a white solid (62%); m.p. 130–131 °C; IR (cm^{-1}): 2230, 1695, 1678, 1672; ^1H NMR ($CDCl_3$): 1.32 (s, 9H), 2.28–2.33 (m, 2H), 3.03–3.11 (m, 2H), 3.26–3.30 (m, 2H), 4.21–4.32 (m, 2H), 4.59–4.66 (m, 1H), 5.29–5.31 (m, 2H), 5.53 (bs, 1H), 6.39 (bs, 1H), 7.07–7.11 (m, 3H), 7.21–7.33 (m, 6H), 7.55 (s, 1H), 7.61 (d, $J = 8.2$ Hz, 2H); MS (CI): 531 (MH^+). Anal. ($C_{29}H_{34}N_6O_4$) C, H, N.

*5.1.2.11. 3-{[1-(4-Cyanobenzyl)-1H-imidazol-5-yl]methyl}-β-Ala-(S)-Phe-NH_2 trifluoroacetate (**A1**).* Carbamate **23** (50 mg, 0.12 mmol) was dissolved in 10 ml of a solution of TFA/CH_2Cl_2 (1:1). The reaction mixture was stirred at room temperature for 4 h. The solvent was then evaporated. The residue was triturated in Et_2O and the white solid was filtered and dried to give **A1** (98%); m.p. 86–89 °C; IR (cm^{-1}): 2230, 1695, 1680; ^1H NMR (DMSO-d_6): 2.69–2.82 (m, 2H), 2.98–3.15 (m, 4H), 4.15–4.35 (m, 2H), 4.38–4.50 (m, 1H), 5.62 (bs, 2H), 7.14 (s, 1H), 7.20–7.25 (m, 7H), 7.40 (d, $J = 8.2$ Hz, 2H), 7.58 (s, 1H), 7.90 (d, $J = 8.2$ Hz, 2H), 8.43 (d, $J = 8.1$ Hz, 1H), 9.05 (bs, 2H); MS (CI): 545 (MH^+). Anal. ($C_{24}H_{26}N_6O_2 \cdot CF_3COOH$) C, H, N.

5.2. Biology

5.2.1. Preparation of FTase from the cytosolic fraction of rat brain [22]

Sprague-Dawley male rats (9–10 weeks old) were sacrificed; brains were removed and immediately placed in an ice-cold 0.1 M HEPES buffer, pH 7.4, 25 mM $MgCl_2$ and 10 mM DTT (dithiothreitol). The brains were cleaned and homogenized in a 0.1 M HEPES buffer, pH 7.4, 1 mM $MgCl_2$ and 1 mM DTT. The homogenates were centrifuged at 10 000 g for 20 min at 4 °C. The supernatants were centrifuged at 100 000 g for 1 h at 4 °C. The cytosolic fraction (the 100 000 g supernatants) was stored at –80 °C. Protein concentration was determined by the bicinchoninic acid (BCA) protein assay

method (Pierce) using bovine serum albumin as protein standard.

5.2.2. Protein prenyl transferase assay

FTase activity was determined by a continuous fluorescence assay (modified by us [20]), as previously described [21]. The data was collected on a Spex Fluoro Max spectrofluorimeter. Optimal parameters are an excitation wavelength at 340 nm and an emission at 505 nm (slit 10,10) for dansyl-CVIM and dansyl-GCVLL. The standard reaction mixture containing 50 mM Tris–HCl, pH 7.5, 5 mM $MgCl_2$, 10 μM $ZnCl_2$, 5 mM DTT, 0.01% *n*-dodecyl-β-D-maltoside, 5.4 mg ml^{-1} of cytosolic protein, 1.3 μM dansyl-CVIM and 25 μM FPP for the FTase assay, and 4 μM dansyl-GCVLL and 10 μM GGPP for the GGT-I assay, was incubated at 25 °C, and fluorescence intensity was recorded for 10 min. A study of cross prenylation of dansyl-CVIM by GGTase with FPP or GGPP was performed. No variation in fluorescence was observed in any case. Graphical representations of fluorescence variation $\Delta F/\Delta t = f$ [ligand] gave sigmoid plots. Analysis of cell curves made it possible to calculate the IC_{50} values of each compound by using a theoretical equation (Graphpad Prism 3.03, Graphpad software, San Diego, CA).

Competitive inhibition patterns were performed as previously described [21] by varying CVIM concentration in the presence of competitor concentration. The mathematical method by Lineweaver and Burk [21] showed unvaried V_{max} and varied K_m.

5.2.3. Cell culture and growth assays

L1210 (murine lymphocytic leukemia), DU145 (human prostate cancer), PC3 (hormone-independent human prostate cancer) and LNCaP (hormone-dependent human prostate cancer) were grown at 37 °C in RPMI 1640 medium supplemented with 10% fetal calf serum, in a humidified incubator containing 5% CO_2. Cells were allowed to grow for 72 h in 96-microwell plates. The cell medium was then changed to serum-free medium and the cells were starved for 24 h for culture synchronization. Cells were then incubated in culture medium containing various concentrations of test compounds (final concentration < 0.1% DMSO). For L1210, cell growth was estimated by numeration and for DU145, PC3 and LNCaP, by the colorimetric MTT test.

5.3. Molecular modeling

Molecular modeling studies were performed using SYBYL software version 6.92 [35] running on a Silicon Graphics workstation. Three-dimensional models of compounds **A1**, **A5** and **A7** were built from a standard fragment library and their geometry was subsequently optimized using the Tripos force field [36] including the electrostatic term calculated from Gasteiger and Hückel atomic charges. Powell's method, available in the Maximin2 procedure, was used for energy minimization until the gradient value was lower than 0.001 kcal mol^{-1} $Å^{-1}$. The structure of human FTase complexed with FPP and the inhibitor **66** described by Bell [37] was obtained from its X-ray crystal structure in the RCSB Protein Data Bank (1LD7). Flexible docking of **A1**, **A5** and **A7** into the enzyme active site was performed using GOLD software [38]. The distance observed in the crystal structure between distal nitrogen imidazole and the zinc cation, was applied as a constraint. For each compound, the most stable docking model was selected from the best conformation predicted by the GoldScore [38] and X-Score [39] scoring functions. The complexes were energy-minimized using the Powell method available in the Maximin2 procedure with the Tripos force field and a dielectric constant of 4.0 until the gradient value reached 0.01 kcal mol^{-1} $Å^{-1}$.

Acknowledgements

The authors are grateful to the "Association pour la Recherche contre le Cancer" for their financial support.

References

[1] D.M. Leonard, J. Med. Chem. 40 (1997) 2971–2990.
[2] J.L. Bos, Cancer Res. 49 (1989) 4682–4689.
[3] K.N. Cho, K.I. Lee, Arch. Pharm. Res. 25 (2002) 759–769.
[4] P. Russo, M. Loprevite, A. Cesario, A. Ardizzoni, Curr. Med. Chem. Anti-Canc. Agents 4 (2004) 123–138.
[5] I.M. Bell, J. Med. Chem. 47 (2004) 1869–1878.
[6] J. Ohkanda, D.B. Knowles, M.A. Blaskovich, S.M. Sebti, A.D. Hamilton, Curr. Top. Med. Chem. 2 (2002) 303–323.
[7] P. Haluska, G.K. Dy, A.A. Adjei, Eur. J. Cancer 38 (2002) 1685–1700.
[8] C. Baum, P. Kirschmeier, Curr. Oncol. Rep. 5 (2003) 99–107.
[9] F. Caponigro, M. Casale, J. Bryce, Expert Opin. Investig. Drugs 12 (2003) 943–954.
[10] S. Rao, D. Cunningham, A. de Gramont, W. Scheithauer, M. Smakal, Y. Humblet, G. Kourteva, T. Iveson, T. Andre, J. Dostalova, A. Illes, R. Belly, J.J. Perez-Ruixo, Y.C. Park, P.A. Palmer, J. Clin. Oncol. 22 (2004) 3950–3957.
[11] B.E. Johnson, J.V. Heymach, Clin. Cancer Res. 10 (2004) 4254s–4257s.
[12] J. Gotlib, Curr. Hematol. Rep. 4 (2005) 77–84.
[13] A.G. Taveras, P. Kirschmeier, C.M. Baum, Curr. Top. Med. Chem. 3 (2003) 1103–1114.
[14] D.J. Augeri, D. Janowick, D. Kalvin, G. Sullivan, J. Larsen, D. Dickman, H. Ding, J. Cohen, J. Lee, R. Warner, P. Kovar, S. Cherian, B. Saeed, H. Zhang, S. Tahir, S.-C. Ng, H. Sham, S.H. Rosenberg, Bioorg. Med. Chem. Lett. 9 (1999) 1069–1074.
[15] R. Millet, J. Domarkas, R. Houssin, P. Gilleron, J.-F. Goossens, P. Chavatte, C. Logé, N. Pommery, J. Pommery, J.-P. Hénichart, J. Med. Chem. 47 (2004) 6812–6820.
[16] S.B. Long, P.J. Casey, L.S. Beese, Nature 419 (2002) 645–650.
[17] N.J. Ede, J. Immunol. Methods 267 (2002) 3–11.
[18] H.M. Geysen, R.H. Meloen, S.J. Barteling, Proc. Natl. Acad. Sci. USA 81 (1984) 3998–4002.
[19] N.J. Maeji, A.M. Bray, R.M. Valerio, M.A. Seldon, J.-X. Wang, H.M. Geysen, Pept. Res. 4 (1991) 142–146.
[20] L. Goossens, S. Deweer, J. Pommery, J.-P. Hénichart, J.-F. Goossens, J. Pharm. Biomed. Anal. 37 (2005) 417–422.
[21] P.B. Cassidy, J.M. Dolence, C.D. Poulter, Methods Enzymol. 250 (1995) 30–43.
[22] S.G. Khan, H. Mukhtar, R. Agarwal, J. Biochem. Biophys. Methods 30 (1995) 133–144.
[23] T.S. Reid, K.L. Terry, P.J. Casey, L.S. Beese, J. Mol. Biol. 343 (2004) 417–433.
[24] M.H. Gelb, W.C. Van Voorhis, F.S. Buckner, K. Yokoyama, R. Eastman, E.P. Carpenter, C. Panethymitaki, K.A. Brown, D.F. Smith, Mol. Biochem. Parasitol. 126 (2003) 155–163.

[25] J. Ohkanda, F.S. Buckner, J.W. Lockman, K. Yokoyama, D. Carrico, R. Eastman, K. de Luca-Fradley, W. Davies, S.L. Croft, W.C. Van Voorhis, M.H. Gelb, S.M. Sebti, A.D. Hamilton, J. Med. Chem. 47 (2004) 432–445.
[26] A. Ryckebusch, P. Gilleron, R. Millet, R. Houssin, A. Lemoine, N. Pommery, P. Grellier, C. Sergheraert, J.-P. Hénichart, Chem. Pharm. Bull. (Tokyo) 53 (2005) 1324–1326.
[27] S.M. Sebti, C.J. Der, Nat. Rev. Cancer 3 (2003) 945–951.
[28] S. Margaritora, A. Cesario, V. Porziella, P. Granone, A. Catassi, P. Russo, Lett. Drug Des. Discov. 2 (2005) 26–35.
[29] M. Wherlock, A. Gampel, C. Futter, H. Mellor, J. Cell Sci. 117 (2004) 3221–3231.
[30] C.L. Gau, J. Kato-Stankiewicz, C. Jiang, S. Miyamoto, L. Guo, F. Tamanoi, Mol. Cancer Ther. 4 (2005) 918–926.
[31] H.R. Ashar, L. James, K. Gray, D. Carr, M. McGuirk, E. Maxwell, S. Black, L. Armstrong, R.J. Doll, A.G. Taveras, W.R. Bishop, P. Kirschmeier, Exp. Cell Res. 262 (2001) 17–27.
[32] C. Falugi, S. Trombino, P. Granone, S. Margaritora, P. Russo, Curr. Cancer Drug Targets 3 (2003) 109–118.
[33] Q. Zeng, X. Si, H. Horstmann, Y. Xu, W. Hong, C.J. Pallen, J. Biol. Chem. 275 (2000) 21444–21452.
[34] K. Jiang, D. Coppola, N.C. Crespo, S.V. Nicosia, A.D. Hamilton, S.M. Sebti, J.Q. Cheng, Mol. Cell. Biol. 20 (2000) 139–148.
[35] SYBYL 6.92, Tripos Associates, Inc., 1699 South Hanley Road, St. Louis, MO 63144.
[36] M. Clark, R.D. III Cramer, N. Van Opdenbosch, J. Comput. Chem. 10 (1989) 982–1012.
[37] I.M. Bell, S.N. Gallichio, M. Abrams, L.S. Beese, D.C. Beshore, H. Bhimnathwala, M.J. Bogusky, C.A. Buser, J.C. Culberson, J. Davide, M. Ellis-Hutchings, C. Fernandes, J.B. Gibbs, S.L. Graham, K.A. Hamilton, G.D. Hartman, D.C. Heimbrook, C.F. Homnick, H.E. Huber, J.R. Huff, K. Kassahun, K.S. Koblan, N.E. Kohl, R.B. Lobell, J.J. Lynch Jr., R. Robinson, A.D. Rodrigues, J.S. Taylor, E.S. Walsh, T.M. Williams, C.B. Zartman, J. Med. Chem. 45 (2002) 2388–2409.
[38] G. Jones, P. Willett, R.C. Glen, A.R. Leach, R. Taylor, J. Mol. Biol. 267 (1997) 727–748.
[39] R. Wang, L. Lai, S. Wang, J. Comput. Aided Mol. Des. 16 (2002) 11–26.